

Room-temperature ultraviolet luminescence from γ -CuCl grown on near lattice-matched silicon

L. O'Reilly,^{a)} O. F. Lucas, P. J. McNally, and A. Reader^{b)}

Nanomaterials Processing Laboratory, Research Institute for Networks and Communications Engineering (RINCE), School of Electronic Engineering, Dublin City University, Dublin 9, Ireland

Gomathi Natarajan, S. Daniels, and D. C. Cameron^{c)}

Nanomaterials Processing Laboratory, National Centre for Plasma Science and Technology (NCPST), School of Electronic Engineering, Dublin City University, Dublin 9, Ireland

A. Mitra, M. Martinez-Rosas,^{d)} and A. L. Bradley

Semiconductor Photonics, Physics Department, Trinity College, Dublin 2, Ireland

(Received 7 June 2005; accepted 24 October 2005; published online 7 December 2005)

We have probed the luminescence properties of a wide-band-gap, direct band-gap optoelectronic material, grown on closely lattice-matched silicon substrates, namely, γ -CuCl on Si. This material system is compatible with current Si or GaAs-based electronic/optoelectronic technologies. Polycrystalline epitaxy of CuCl can be controlled such that it maintains an orientation similar to the underlying Si substrate. Importantly, chemical interactions between CuCl and Si are eliminated. Photoluminescence and cathodoluminescence results for CuCl, deposited on either Si (100) or Si (111), reveal a strong room-temperature Z_3 excitonic emission at ~ 387 nm. We have developed and demonstrated the room-temperature operation of an ultraviolet electroluminescent device fabricated by the growth of γ -CuCl on Si. The application of an electrical potential difference across the device results in an electric field, which promotes light emission through hot-electron impact excitation of electron-hole pairs in the γ -CuCl. Since the excitonic binding energy in this direct band-gap material is of the order of 190 meV at room temperature, the electron-hole recombination and subsequent light emission at ~ 380 and ~ 387 nm are mediated by excitonic effects. © 2005 American Institute of Physics. [DOI: 10.1063/1.2138799]

I. INTRODUCTION

GaN and its related alloys have become synonymous with blue-violet and ultraviolet light-emitting and laser diodes.¹ The ability to fabricate devices emitting in this portion of the electromagnetic spectrum is the result of the large direct band gap in these III-nitride alloys (3–6 eV). These materials also possess high electron mobilities, high breakdown electric fields, and good thermal conductivities. A number of years ago Nakamura and Fasol,² Itaya *et al.*,³ and Bulman *et al.*⁴ demonstrated the room-temperature violet laser emission in AlGaIn/GaN/AlGaIn-based heterostructures under pulsed and continuous-wave (cw) operations. However, these early devices were plagued by the presence of numerous threading dislocations (TDs), which impacted severely on the lifetimes and optical performance of laser diodes in particular. These densities reached values as high as $\sim 10^{10}$ cm⁻², and were due mainly to the severe lattice mismatch between the substrate materials (e.g., 6H-SiC or α -Al₂O₃) and the grown III-nitride epilayers (mismatches as high as 13.6% in the GaN/Al₂O₃ system⁵).

The recent introduction of epitaxial lateral overgrowth (ELOG) techniques^{6,7} has facilitated the production of III-nitride films with threading dislocation densities reduced by three to four orders of magnitude with respect to conventional metal-organic chemical-vapor deposition techniques on both sapphire and SiC substrates. Recent studies of the optical properties of ELOG GaN and InGaIn quantum wells^{8,9} have revealed that TDs act as nonradiative recombination centers. The minority-carrier diffusion length (<200 nm) is smaller than the average distance between the TDs, such that the emission mechanisms of the carriers that do combine radiatively appear to be unaffected by moderate TD densities ($\sim 10^6$ – 10^9 cm⁻²).¹⁰ However, reducing the TD density has been shown to reduce the reverse leakage current by ~ 3 orders of magnitude in GaN *p-n* junctions,¹¹ InGaIn single-quantum well¹² and multiple-quantum-well light-emitting diodes¹³ (LEDs), and GaN/AlGaIn heterojunction field-effect transistors¹⁰ fabricated on ELOG GaN. The use of ELOG GaN has also resulted in marked improvements in the lifetime of InGaIn/GaN laser diodes.⁶ Recently, other researchers have investigated the lateral growth of GaN films suspended from {11 $\bar{2}$ 0} side walls of [0001]-oriented GaN columns into and over adjacent etch walls using the metal-organic vapor-phase epitaxy (MOVPE) technique, without the use of, or contact with, a supporting mask or substrate (as in ELOG).^{14,15} This technique became known as *pendeoeptaxy* and it also serves to reduce TD densities to 10^4 – 10^5 cm⁻²—many orders of magnitude lower, but still

^{a)}Electronic mail: oreillyl@eeng.dcu.ie

^{b)}Present address: Innos Ltd., Faculty of Electronics & Computing, University of Southampton, Highfield, Southampton SO17 1BJ, UK.

^{c)}Present address: Advanced Surface Technology Research Laboratory (ASTRaL), Lappeenranta University of Technology, P.O. Box 181, 50101 Mikkeli, Finland.

^{d)}Also at the Universidad Autónoma de Baja California, Ensenada, Mexico.

very high compared to mature technologies such as Si or GaAs.

In the past few years a number of researchers have attempted to integrate III-nitride epilayers with a Si substrate. One favored substrate has been Si (111), as this surface has a 120° symmetry which is somewhat compatible with the hexagonal III nitrides, and Si possesses obvious advantages for compatibility with integrated devices and circuits, has good thermal conductivity, and would be a low cost alternative.^{16–18} This route is proving difficult, as the difference in lattice parameters and the strength of the Si–N bond prevent the formation of smooth, single-crystal GaN on Si (111).^{18,19} To some extent this has been alleviated by using a two-step method involving various buffer layers such as SiC,^{20,21} AlN,^{22,23} GaAs,²⁴ AlAs,²⁵ and SiN_x.²⁶ These typically yield smooth morphologies and columnar microstructures with a TD density of 10¹⁰–10¹¹ cm⁻²—no real advance. The principal weakness of these approaches lies in the fact that the additional heteroepitaxial layer does not necessarily alleviate mismatch problems due to the fundamental incompatibility of hexagonal III nitrides and cubic Si or GaAs. A bottom line has emerged: the reduction of deleterious threading dislocations in wide-band-gap materials for optoelectronics devices is essential to their operation, and, in particular, to their longevity. Specifically, the lattice mismatch between the substrate materials and the overgrown epilayers is the main issue to be resolved.

An alternative approach is addressed in this paper: the *growth* and *development* of an electroluminescent device consisting of cubic γ -CuCl (a wide- and direct band-gap semiconductor) on low lattice-mismatched cubic Si. Research on the cuprous halides has focused on three main thrusts over the past decade: (1) spectroscopic and theoretical studies of band structures and excitonic-based luminescence in CuCl and CuBr,^{27–31} (2) fundamental photoluminescence studies of CuCl quantum dots/nanocrystals embedded in NaCl crystals,^{32–34} and (3) fundamental surface studies of the growth mechanisms involved in the heteroepitaxy of CuCl single crystals on a number of substrates.^{35–40} One group of researchers has examined the surface growth mechanisms in the heteroepitaxy of CuCl on both Si and GaAs substrates by molecular-beam epitaxy.⁴⁰ Again, this study focused on the fundamental physics of the island growth process and the nature of the interfacial bonding. In our work, we progress on these studies by moving into the realm of producing light-emitting devices.

The cuprous halides, e.g., CuCl, CuBr, and CuI, are ionic I–VII compounds with the zinc-blende (T_d^2 and $F\bar{4}3m$) structure^{29,36} at room temperature.^{31,41} At room temperature, the prevalent phase of CuCl is called γ -CuCl, which is a direct band-gap cubic semiconductor, with a band gap of $E_G=3.395$ eV ($\lambda \sim 365$ nm—blue/violet light) and a lattice constant $a_{\text{CuCl}}=0.541$ nm.^{42,43} Given that the lattice constant for cubic Si is $a_{\text{Si}}=0.543$ nm (room temperature),⁴² this implies that the lattice misfit of CuCl is $<0.4\%$ with respect to Si (100) at room temperature. This low mismatch with respect to Si implies that γ -CuCl is a promising candidate for low defect density heteroepitaxy on Si. (The ionicity of CuCl is 0.75, while that of GaAs and Si is 0.31 and 0, respectively,

which suggests that studies of growth of γ -CuCl on GaAs may also be profitable as the lattice mismatch is $\sim 4\%$.⁴⁰) Finally, the excitonic properties of copper halides have attracted much attention, as the exciton binding energies (190 meV for CuCl and 108 meV for CuBr) are much larger than those for III–V and II–VI semiconductors.²⁸

II. EXPERIMENTAL DETAILS

Prior to deposition of CuCl layers the silicon substrates were degreased in organic solvents and the native oxide was removed by dipping in a hydrofluoric acid solution. The substrates were then rinsed in de-ionized water and blown dry with a nitrogen gun. Commercially supplied CuCl powders with purities of 97% (Merck) and 99.999% (Alfa Aesar), respectively, were heated in a quartz crucible and the evaporation rate, which was controlled by monitoring the frequency of a crystal oscillator, was approximately 0.5 nm s⁻¹. The evaporator was an Edwards 306A thermal resistance evaporator with a base pressure of $\sim 1 \times 10^{-6}$ mbar.

X-ray-diffraction (XRD) measurements, to investigate the crystallinity of the thin films, were performed using a D8 Advance, x-ray diffractometer from Bruker Advanced X-ray Solutions. The x rays were monochromatic with a wavelength of 1.54 Å, characteristic of a Cu target. Bragg-Brentano geometry was used to investigate the bulk of the film. The resolution of the diffraction patterns is 0.01°.

UV/Vis spectra were recorded on a Perkin Elmer Lambda 40 UV/Vis spectrometer at room temperature with a resolution of 1 nm.

An UV Ar-ion Inova laser with a second-harmonic generation beta barium borate (BBO) crystal producing a 244 nm line was used to excite photoluminescence (PL), which was captured with a TRIAX 190 Jobin Yvon-Horiba spectrometer (resolution of 0.3 nm) with liquid-nitrogen-cooled charge-coupled device (CCD) detector. The maximum excitation power was ~ 10 W/cm². Temperature-dependent measurements were performed from room temperature to 10 K.

Room-temperature cathodoluminescence (CL) studies were performed using a LEO Stereoscan 440 scanning electron microscope with an electron beam of 10 keV and probe current of 15 nA. The luminescence was collected by a parabolic mirror, with high collection efficiency ($\sim 80\%$), placed 1 mm above the sample. The signal collected was transferred onto a Gatan MonoCL instrument equipped with a 1200 lines/mm grating. The spectral resolution was approximately 1 nm.

For the electroluminescent device (ELD) the γ -CuCl/Si films were immediately mounted on a dip coater and a commercially available polysilsesquioxane (PSSQ)-based solution made by the Emulsitone® incorporation (USA) was used as the capping layer. The γ -CuCl/Si structure was immersed in PSSQ solution at room temperature for approximately 15 min. After withdrawing, it was dried in air for 5 min, and then baked in vacuum at a temperature of 150 °C for 1 h. The thickness of the capping layer was estimated to be ~ 350 nm using a stylus profilometer.

The electroluminescence measurements of the test de-

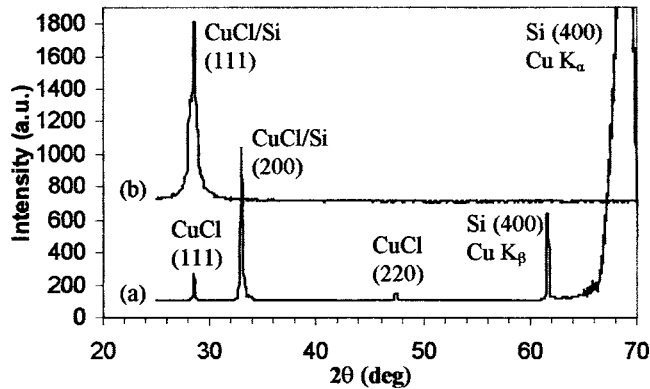


FIG. 1. X-ray θ - 2θ diffraction pattern of γ -CuCl (a) grown on a Si (100) substrate and (b) on a Si (111) substrate.

vices were evaluated using a SOFIE spectrophotometer with a photomultiplier tube (spectral range of 200–900 nm). The ELD device was driven by an ac sinusoidal wave form with a frequency of 1 kHz and a peak-to-peak voltage of 100 V.

III. RESULTS AND DISCUSSION

In order to verify that one can controllably grow polycrystalline γ -CuCl on Si (111) and Si (100) substrates, CuCl thin-film samples with typical layer thicknesses of ~ 500 nm were grown on Si (100), Si (111), and glass substrates at room temperature using a vacuum deposition method at a base pressure of $\sim 1 \times 10^{-6}$ mbar.

Immediately following deposition of CuCl on these substrates XRD measurements were performed to monitor the crystallinity of the deposited CuCl thin films. These XRD scans were then compared to the standard powder-diffraction files and to the pattern from the starting CuCl powder, which was compressed into a pellet. Indexing of the interplanar spacings using the Bragg equation for the cubic unit cell, $h^2 + k^2 + l^2 = (4a^2/\lambda^2)\sin^2 \theta$, (where h , k , and l are the Miller indices, a is the lattice constant, λ is the incident radiation wavelength, and θ is the Bragg angle) confirmed that the γ -CuCl was in the cubic zinc-blende form as expected at room temperature. Glass is an amorphous substrate and therefore should have no influence on the crystal orientation of a thin film grown upon it. The evaporated CuCl film on glass was strongly oriented in the $\langle 111 \rangle$ direction, which confirms that this is the preferred growth direction of the CuCl. XRD patterns were taken in the Bragg-Brentano geometry of CuCl deposited on Si (100) and Si (111) substrates, as shown in Fig. 1 curves (a) and (b), respectively. An offset has been applied to the spectra for clarity. Due to the very small difference in lattice constant of γ -CuCl and Si, the Bragg peaks appear at similar 2θ values in the XRD spectra. The data confirmed that on the Si (111) the γ -CuCl grows epitaxially in the $\langle 111 \rangle$ direction and some growth in the $\langle 100 \rangle$ direction is evident on a Si (100) substrate. Further details of the XRD measurements have been published elsewhere.⁴⁴

One challenge associated with the use of CuCl is that it is sensitive to air and/or moisture. Under the influence of light and moisture, hydrated oxyhalides of Cu^{++} are formed.⁴¹ This reaction can be easily recognized by a color change in CuCl associated with the presence of the greenish

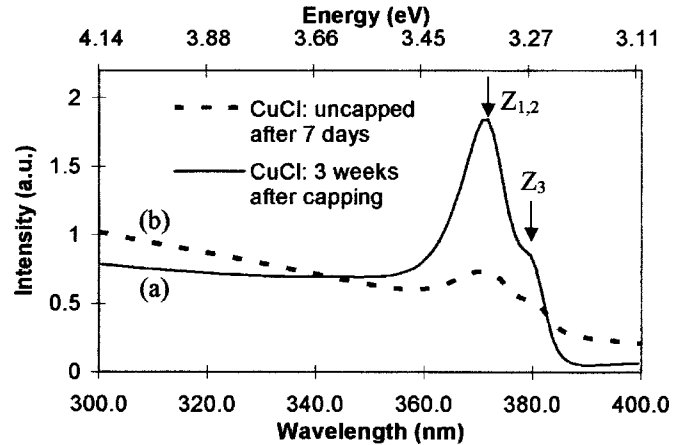


FIG. 2. UV-Vis absorption spectrum of γ -CuCl on quartz: (a) capped CuCl 3 weeks after deposition and (b) uncapped CuCl 7 days after deposition.

color produced by Cu^{++} ions. A protective layer is required to prevent this reaction. This layer consists of a dip-coated liquid-glass layer, which Fourier transform infrared (FTIR) analysis has shown to be an effective means of sealing the CuCl system for many months.

We have previously shown room-temperature UV-Vis absorption spectra of γ -CuCl thin films on a quartz substrate measured immediately after deposition.⁴⁴ Figure 2, curve (a) shows the absorption spectrum of a liquid-glass-capped CuCl layer measured 3 weeks after deposition. The main peak results from the contribution of both high- and low-energy excitonic bands, historically called the $Z_{1,2}$ and Z_3 excitons, respectively. The $Z_{1,2}$ and Z_3 excitons originate from the coupling of the lowest conduction-band state Γ_6 to both the uppermost valence-band holes Γ_8 ($Z_{1,2}$) and Γ_7 (Z_3), respectively.^{28,45} The energy values of 3.34 eV ($\lambda \sim 372$ nm) for the $Z_{1,2}$ exciton and 3.27 eV ($\lambda \sim 380$ nm) for the Z_3 exciton are in close agreement with the values reported by other authors for room-temperature CuCl absorption measurements.^{45,46} The absorption spectrum of an uncapped CuCl sample measured 7 days after deposition is shown in Fig. 2, curve (b). The drastic decrease in the intensity of the exciton peak compared to the capped sample illustrates that the CuCl optical quality degrades due to air/moisture absorption. The presence of the excitonic peaks in the capped sample several weeks after deposition provides further proof that the CuCl is fully protected by the liquid-glass coating which is also transparent to ultraviolet and visible light at the wavelengths of interest.

A PL spectrum measured at 10 K for a CuCl on Si (100) sample, grown from CuCl powder of 99.999% purity, is shown in Fig. 3(a). Four peaks are evident in the spectrum. The peak which occurs at ~ 3.212 eV ($\lambda \sim 387$ nm) is the Z_3 free exciton peak. Due to the large binding energy of the free exciton (~ 190 meV), this peak was also clearly evident in room-temperature PL measurements at an energy $E = 3.236$ eV ($\lambda \sim 384$ nm) shown in the inset of Fig. 3(a). On the low-energy side of the free exciton, a peak occurs at ~ 3.189 eV ($\lambda \sim 389.8$ nm). This is attributed to an emission from an exciton bound to an impurity,^{28,47} which has been called the I_1 bound exciton. The impurity has previously

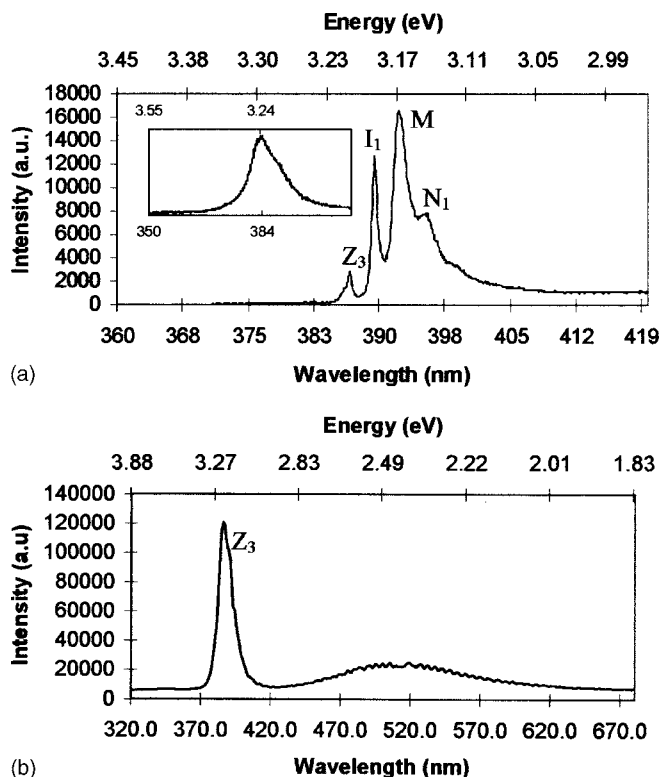


FIG. 3. (a) Photoluminescence spectrum of CuCl on Si (100) at 10 K, (inset: PL spectrum at room temperature) and (b) room-temperature cathodoluminescence spectrum of CuCl on Si (100).

been identified as a neutral acceptor, possibly a Cu vacancy.⁴⁸ A third peak, which appears at 3.166 eV ($\lambda \sim 392.7$ nm), is identified as a free biexciton M . The free biexciton results from exciton-exciton collisions resulting in the formation of an excitonic molecule (so-called biexciton).²⁸ At 3.141 eV ($\lambda \sim 395.7$ nm) a fourth peak labeled N_1 is evident, and likely originates from a biexciton bound to an impurity. Similar to the I_1 bound exciton, the most probable candidate for the impurity is considered to be a neutral acceptor.²⁸

The main features of the room-temperature CL spectrum [Fig. 3(b)] include a strong emission at $\lambda \sim 387$ nm (3.21 eV) and a broad blue-green emission band centered at ~ 520 nm (2.39 eV). This broadband occurred in samples with starting CuCl powders of both 97% and 99.999% purities but its exact origin has yet to be determined. The emission at 3.21 eV agrees reasonably well with the values reported in the literature for the Z_3 free exciton emission.^{28,49}

A cross-sectional view of the ELD structure is shown in Fig. 4. The aims in developing this structure were to confirm

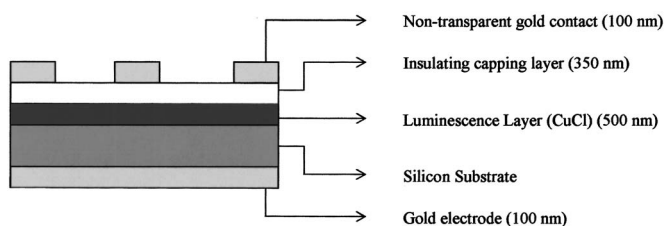


FIG. 4. The γ -CuCl on Si electroluminescent device fabricated in this study.

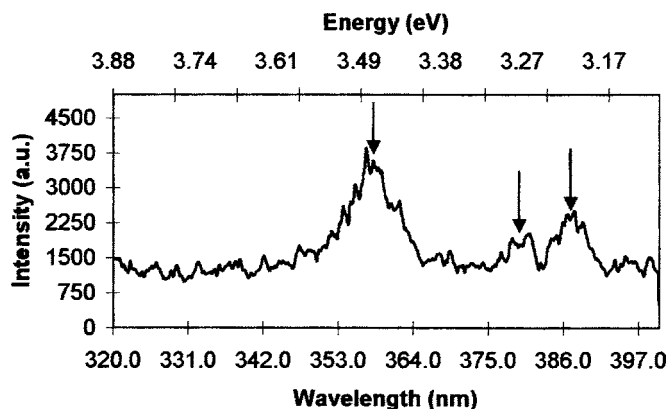


FIG. 5. A plot of electroluminescence output intensity as a function of wavelength at room temperature.

the compatibility of γ -CuCl with Si, to confirm that no deleterious CuCl-Si interaction occurs during device fabrication, and to demonstrate UV light emission upon a lattice-matched Si substrate. A gold Ohmic contact layer was deposited on the unpolished side of a p -type silicon substrate. The γ -CuCl was deposited on the polished side of the prepared silicon wafer by thermal evaporation, as previously described.⁴⁴ The insulating/capping layer of SiO₂ was deposited over the CuCl layer by dip coating. The structure was subsequently annealed at 150 °C for 1 h in vacuum. Gold contacts were fabricated above this layer by sputtering. In this metal-insulator-semiconductor (MIS) structure, light emission occurs through hot-electron impact excitation of electron-hole pairs. As the Au electrode was nontransparent, electroluminescence (EL) emission was observed principally from the edges of the electrode; hence the intensity of the spectrum is rather low. The main feature of the spectrum (Fig. 5) is a broadband centered on 359 nm (3.46 eV) probably due to emission from the direct band-to-band transition. Two further peaks can be identified at ~ 380 nm (3.27 eV) and ~ 387 nm (3.21 eV). The peak at ~ 387 nm agrees with the Z_3 excitonic emission also seen in room-temperature CL measurements as already discussed, and the separation of the peaks of approximately 60 meV is consistent with that of the $Z_{1,2}$ and Z_3 excitons observed in room-temperature UV-Vis absorption measurements. Therefore the emission at ~ 380 nm can be tentatively assigned to a $Z_{1,2}$ excitonic emission.

IV. CONCLUSION

In summary, we have grown polycrystalline closely lattice-matched γ -CuCl on Si (111) and Si (100) substrates. CuCl grows preferentially in the $\langle 111 \rangle$ direction but some epitaxial growth also occurs on a Si (100) substrate. PL and CL reveal a strong room-temperature Z_3 excitonic emission at ~ 387 nm. The application of an electrical potential difference across a MIS structured electroluminescent device results in an UV light emission. Since the excitonic binding energy in this direct band-gap material is of the order of 190 meV at room temperature, the electron-hole recombination and subsequent light emission at ~ 380 and ~ 387 nm

are mediated by excitonic effects. This opens up possibilities for UV optoelectronics on lattice-matched silicon substrates.

ACKNOWLEDGMENT

This project is funded by the Irish Research Council for Science Engineering and Technology (IRCSET) Grant No. SC/02/7.

- ¹B. Metzger, *Compound Semicond.* **7**, 57 (2001).
- ²S. Nakamura and G. Fasol, *The Blue Laser Diode: GaN Based Light Emitters and Lasers* (Springer, Berlin, 1997).
- ³K. Itaya *et al.*, *Jpn. J. Appl. Phys., Part 2* **35**, L1315 (1996).
- ⁴G. E. Bulman *et al.*, *Electron. Lett.* **33**, 1556 (1997).
- ⁵O. Ambacher, *J. Phys. D* **31**, 2653 (1998).
- ⁶S. Nakamura *et al.*, *Appl. Phys. Lett.* **72**, 211 (1998).
- ⁷T. S. Zheleva, O.-H. Nam, M. D. Bremser, and R. F. Davis, *Appl. Phys. Lett.* **71**, 2472 (1997).
- ⁸J. A. Freitas, O.-H. Nam, R. F. Davis, G. V. Sagarin, and S. K. Obyden, *Appl. Phys. Lett.* **72**, 2990 (1998).
- ⁹X. Li, S. G. Bishop, and J. J. Coleman, *Appl. Phys. Lett.* **73**, 1179 (1998).
- ¹⁰H. Marchand *et al.*, *MRS Internet J. Nitride Semicond. Res.* **4**, 2 (1999); <http://nsr.mij.mrs.org/4/2/>
- ¹¹P. Kozodoy, J. P. Ibbetson, H. Marchand, P. T. Fini, S. Keller, J. S. Speck, S. P. DenBaars, and U. K. Mishra, *Appl. Phys. Lett.* **73**, 975 (1998).
- ¹²T. Mukai, K. Takekawa, and S. Nakamura, *Jpn. J. Appl. Phys., Part 2* **37**, L839 (1998).
- ¹³C. Sasaoka, H. Sunakawa, A. Kimura, M. Nido, A. Usui, and A. Sakai, *J. Cryst. Growth* **189/190**, 61 (1998).
- ¹⁴T. S. Zheleva, S. A. Smith, D. B. Thomson, K. J. Linthicum, P. Rajagopal, and R. F. Davis, *J. Electron. Mater.* **28**, L5 (1999).
- ¹⁵T. Gehrke, K. J. Linthicum, D. B. Thomson, P. Rajagopal, A. D. Batchelor, and R. F. Davis, *MRS Internet J. Nitride Semicond. Res.* **4S1**, G3.2 (1999); <http://nsr.mij.mrs.org/4S1/G3.2/>
- ¹⁶A. Osinsky *et al.*, *Appl. Phys. Lett.* **72**, 551 (1998).
- ¹⁷K. S. Stevens, M. Kinniburgh, and R. Beresford, *Appl. Phys. Lett.* **66**, 3518 (1995).
- ¹⁸T. L. Chu, *J. Electrochem. Soc.* **118**, 1200 (1971).
- ¹⁹H. M. Manasevit, F. M. Erdmann, and W. I. Simpson, *J. Electrochem. Soc.* **118**, 1864 (1971).
- ²⁰T. Takeuchi, H. Amano, K. Hiramatsu, N. Sawaki, and I. Akasaki, *J. Cryst. Growth* **115**, 634 (1991).
- ²¹A. J. Steckl, J. Devrajan, C. Tran, and R. A. Stall, *Appl. Phys. Lett.* **69**, 2264 (1996).
- ²²S. Guha and N. A. Bojarczuk, *Appl. Phys. Lett.* **72**, 415 (1998).
- ²³P. Kung, A. Saxler, X. Zhang, D. Walker, T. C. Wang, I. Ferguson, and M. Razeghi, *Appl. Phys. Lett.* **66**, 2958 (1995).
- ²⁴J. W. Yang *et al.*, *Appl. Phys. Lett.* **69**, 3566 (1996).
- ²⁵N. P. Kobayashi, P. D. Dapkus, W. J. Choi, A. E. Bond, X. Zhang, and D. H. Rich, *Appl. Phys. Lett.* **71**, 3569 (1997).
- ²⁶Y. Nakada, I. Aksenov, and H. Okumura, *Appl. Phys. Lett.* **73**, 827 (1998).
- ²⁷M. Nakayama, A. Soumura, K. Hamasaki, H. Takeuchi, and H. Nishimura, *Phys. Rev. B* **55**, 10099 (1997).
- ²⁸M. Nakayama, H. Ichida, and H. Nishimura, *J. Phys.: Condens. Matter* **11**, 7653 (1999).
- ²⁹B. Wyncke and F. Bréhat, *J. Phys.: Condens. Matter* **12**, 3461 (2000).
- ³⁰H. Heireche, B. Bouhafs, H. Aourag, M. Ferhat, and M. Certier, *J. Phys. Chem. Solids* **59**, 997 (1998).
- ³¹B. Bouhafs, H. Heirache, W. Sekkal, H. Aourag, and M. Certier, *Phys. Lett. A* **240**, 257 (1998).
- ³²Y. Masumoto and S. Ogasawara, *J. Lumin.* **87–89**, 360 (2000).
- ³³M. Ikezawa and Y. Masumoto, *J. Lumin.* **87–89**, 482 (2000).
- ³⁴J. Zhao, M. Ikezawa, A. V. Fedorov, and Y. Masumoto, *J. Lumin.* **87–89**, 525 (2000).
- ³⁵A. Yanase and Y. Segawa, *Surf. Sci.* **329**, 219 (1995).
- ³⁶A. Yanase and Y. Segawa, *Surf. Sci.* **367**, L1 (1996).
- ³⁷A. Yanase and Y. Segawa, *Surf. Sci.* **357–358**, 885 (1996).
- ³⁸Q. Guo, L. Gui, and N. Wu, *Appl. Surf. Sci.* **99**, 229 (1996).
- ³⁹C. T. Lin, E. Schönherr, A. Schmeding, T. Ruf, A. Göbel, and M. Cardona, *J. Cryst. Growth* **167**, 612 (1996).
- ⁴⁰N. Nishida, K. Saiki, and A. Koma, *Surf. Sci.* **324**, 149 (1995).
- ⁴¹C. Schwab and A. Goltzené, *Prog. Cryst. Growth Charact.* **5**, 233 (1982).
- ⁴²H. G. Grahn, *Introduction to Semiconductor Physics* (World Scientific, Singapore, 1999).
- ⁴³NIST Chemistry Webbook, <http://webbook.nist.gov>
- ⁴⁴L. O'Reilly *et al.*, *J. Mater. Sci.: Mater. Electron.* **16**, 415 (2005).
- ⁴⁵A. Goldmann, *Phys. Status Solidi B* **81**, 9 (1977).
- ⁴⁶G. Suyal, M. Mennig, and H. Schmidt, *J. Mater. Chem.* **10**, 3136 (2002).
- ⁴⁷D. K. Shuh and R. S. Williams, *Phys. Rev. B* **44**, 5827 (1991).
- ⁴⁸M. Certier, C. Wecker, and S. Nikitine, *J. Phys. Chem. Solids* **30**, 2135 (1969).
- ⁴⁹T. Goto, T. Takahashi, and M. Ueta, *J. Phys. Soc. Jpn.* **24**, 314 (1968).